Received: 25 August 2021 | Revised: 8 September 2021 | Accepted: 13 September 2021

DOI: 10.1002/jmr.2938

RESEARCH ARTICLE

Journal of Molecular Recognition WILEY

Identification of DNA methylation by novel optical genosensing: A new platform in epigenetic study using biomedical analysis

Mina Adampourezare[1,2] | Gholamreza Dehghan[1] | Mohammad Hasanzadeh[2,3] | Mohammad-Ali Hosseinpoure Feizi[1,3]

[1]Department of Animal Biology, Faculty of Natural Science, University of Tabriz, Tabriz, Iran

[2]Pharmaceutical Analysis Research Center, Tabriz University of Medical Sciences, Tabriz, Iran

[3]Nutrition Research Center, Tabriz University of Medical Sciences, Tabriz, Iran

Correspondence
Gholamreza Dehghan, Department of Animal Biology, Faculty of Natural Science, University of Tabriz, Tabriz, Iran.
Email: dehghan2001d@yahoo.com

Mohammad Hasanzadeh, Pharmaceutical Analysis Research Center, Tabriz University of Medical Sciences, Tabriz, Iran.
Email: hasanzadehm@tbzmed.ac.ir

Funding information
University of Tabriz of Medical Science; University of Tabriz

Abstract

Due to the important role of methylation in cancer, the use of sensitive analytical methods for early diagnosis and efficient clinical pharmacotherapy is highly demanded. In this study, an innovative label-free method has been developed for the recognition of methylated DNA in the promoter area of adenomatous polyposis coli gene (APC gene). Also, differentiation of unmethylated DNA (GCGGAGTGCGGGTC GGGAAGCGGA) from methylated cDNA (GC(M)GGAGTGC(**M**)GGGTC(**M**)GGGA AGC(**M**)GGA) was performed using optical synthesized probe (thionine-based polymer). Hybridization of pDNA (TCCGCTTCCCGACCCGCACTCCGC) with various types of cDNA sequences was studied by UV-visible and fluorescence spectroscopy. Also, some of the mismatch sequences {(GC(M)GGAGTAC(**M**)GGGTC(M)GGGAAGC (M)GGA) and (GCGGAGTACGGGTCGGGAAGCGGA)} were applied as negative control. For this purpose, The synthesized optical probe was characterized by transmission electron microscopy, atomic force microscopy, dynamic light scattering, zeta potential, energy dispersive X-ray spectroscopy, Fourier transform infrared spectroscopy, UV-Vis, and fluorescence spectroscopy. Under optimal conditions, the analytical performance of engineered DNA-based assay was studied and exhibited excellent dynamic range (1 zM to 3 pM) with low limit of quantitation (LLOQ) of 1 zM. The designed DNA-based assay showed a high capability of discriminating methylation, unmethylated and mismatched sequences. The engineered genosensor is simple and inexpensive and can detect DNA methylation with high sensitivity. Therefore, the designed geno-assay could detect DNA methylation significantly and discriminate from unmethylated DNA. It is expected that the proposed geno-assay could be used for the detection of DNA methylation, genetic mutations, epigenetic alterations, and early stage diagnosis of various cancer toward efficient clinical pharmacotherapy.

KEYWORDS
biomedical analysis, biosensor, DNA methylation, epigenetic, genetic mutations

1 | INTRODUCTION

Cancer refers to a group of diseases that cause abnormal cell growth and division with the potential to invade or spread to other parts of the body. Cancer development is a complex and multifactorial process characterized mainly by genetic mutations and epigenetic alterations.[1]

Epigenetics is defined as heritable alterations in gene expression without alteration in DNA nucleotide sequences.[2] DNA methylation is one of the most common epigenetic modifications resulting from the chemical addition of a methyl group to the cytosine base in the 5′ position in the CpG dinucleotides. The most important and best known epigenetic modification happens in the CpG dinucleotides located in the promoter region[3] that can lead to altered expression of multiple genes, gene silencing, and finally drug resistance and cancer.[4] Gene expression inhibition can be performed either by the binding of transcription factors or through the recruitment of the methyl binding domain (MBD) proteins and other chromatin factors, which will induce a closed state of the chromatin (heterochromatin) and suppress transcription.[5,6]

The APC protein, as a product of the APC gene, acts as a tumor suppressor. This protein prevents cells from uncontrolled growth and division. In addition to controlling cell growth and division, this protein controls attachment of a cell to other cells within a tissue, as well as the movement of cells into or away from the tissue. It also controls the accuracy of the number of chromosomes following cell division. APC protein performs these activities with the help of other proteins involved in signaling and cellular binding.

In recent years, several methods have been used to determine the status of methylation of genes such as methylation-specific PCR by bisulfite conversion, methyl-sensitive restriction enzyme PCR (MSRE-PCR), whole-genome bisulfite sequencing denaturing, high-performance liquid chromatography (DHPLC), isotope-labeled S-adenosylmethionine (SAM), immune reactions, etc.[7-11] These approaches need bisulfite conversion or restriction enzymes for specific modification of DNA bases,[12,13] antibodies, and proteins that bind to cytosine[14-17] or for some specific chemical changes such as bisulfite conversion.[18] Most of these methods are costly and time-consuming. Also, these methods require a lot of solutions and DNA. On the other hand, bisulfite treatment causes DNA degradation. Therefore, nanobiosensing has been developed, which is recognized as an excellent alternative method due to their rapid response, cost-effectiveness, being more sensitive and selective in addition to easy applications as a rapid test in decision-making. Currently, finding direct detection of DNA sequences without using chemical or enzymatic treatments is the area of interest for scientific communities and industries. Designing a DNA nanobiosensor based on fluorescent detection can be a good suggestion for its high sensitivity and high selectivity.[19-23]

In this research, for the first time, a fluorometric nanobiosensor has been designed for DNA methylation assay based on thionine/oxalate polymer. Thionine, (3,7-Diamino-5-phenothiazinium) (TH) (Figure 1A), one of the components of this nanobiosensor, is a

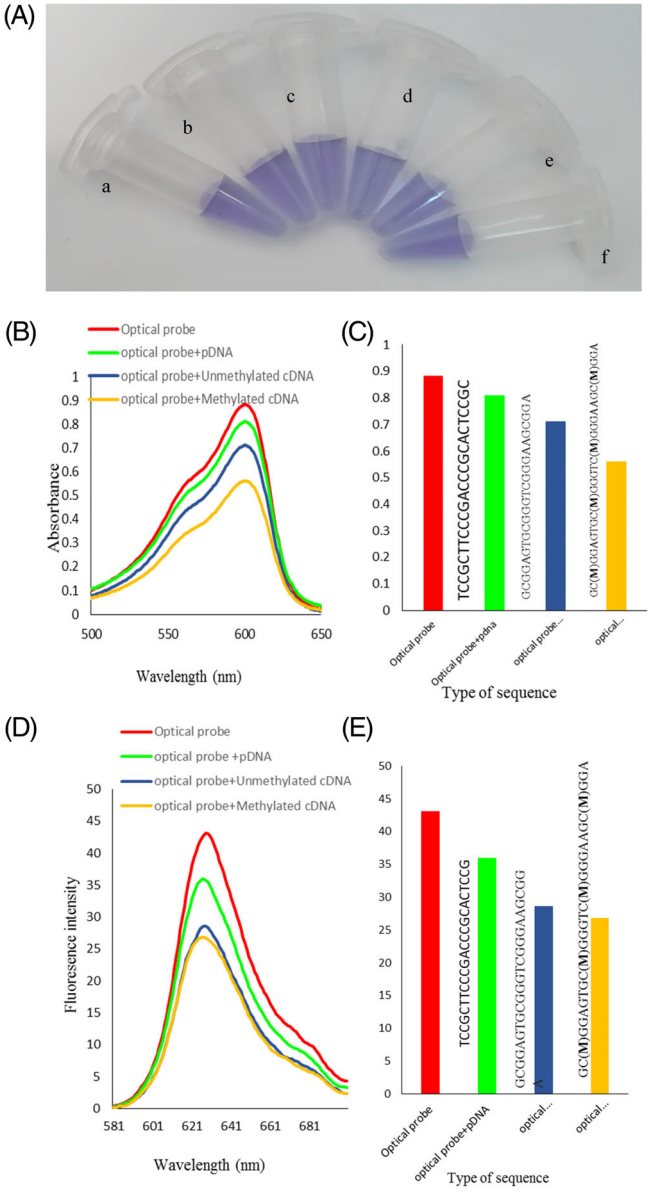

FIGURE 1 A, (a) Color of the optical probe, (b) optical probe +pDNA, (c) optical probe+ unmethylated cDNA, (d) optical probe +unmethylated interfering cDNA, (e) optical probe+ methylated cDNA, (f) optical probe+methylated interfering cDNA,B, UV-Vis of the optical probe, pDNA and hybridization of pDNA with methylated cDNA, methylated interfering cDNA, unmethylated cDNA, unmethylated interfering CDNA, C, Histograms of peak intensity vs type of sequence

cationic tricyclic heteroaromatic molecule. TH contains one heterocyclic nitrogen atom and two amine groups symmetrically distributed on each side and an aromatic central ring system, which is responsible for intense π-π transition absorption bands.[24] Thionine has been studied for its intercalative interaction, photoinduced mutagenic actions on binding to DNA, photoinduced inactivation of viruses, and as impedance-based DNA biosensor.[25-28] Thionine intercalates and also bounds to the outside of linear duplex DNA.[29] Thionine exists in two

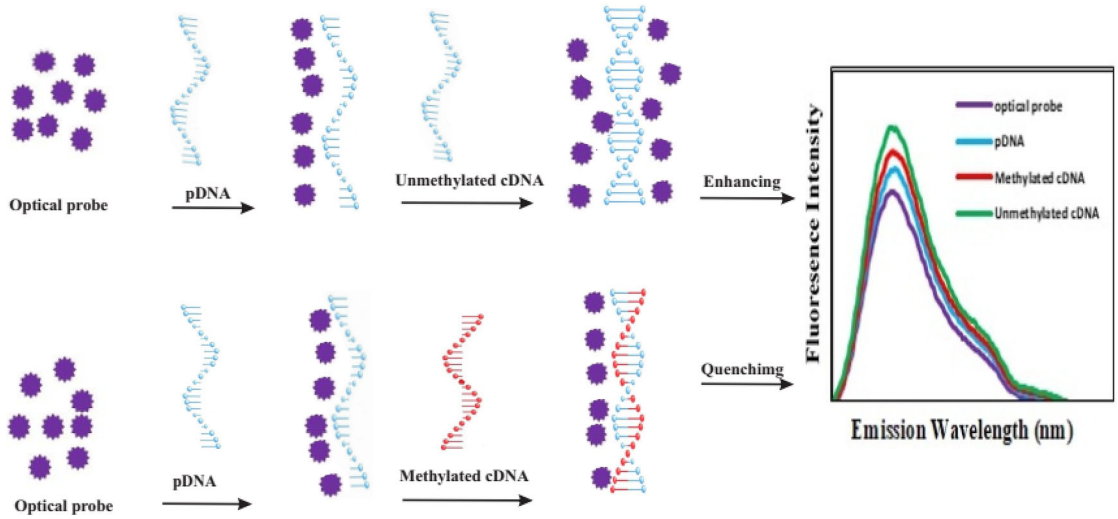

SCHEME 1 Schematic diagram of genosensor preparation steps for DNA methylation assay

different tautomeric forms, and the amino form is intercalated while the imino form is not.[30-32] The UV-Vis spectrum of thionine exhibits two characteristic absorption bands at 598 and 565 nm. The 598 nm band is a characteristic absorption feature of monomeric form, and the 565 nm shoulder can be attributed to the H-type dimer aggregate.[33] In the current study, the thionine/oxalate polymer has been used as a fluorescence probe to distinguish methylated and unmethylated DNA sequences and to detect mismatch through different fluorescence behavior. An overview of the detection mechanism is illustrated in Scheme 1.

Due to the important role of methylation in cancer, the use of sensitive methods for early diagnosis and clinical pharmacotherapy is highly demanded. In this study, an innovative label-free method has been developed for the recognition of methylated DNA in promoter area of adenomatous polyposis coli gene (APC gene). Also, differentiation of unmethylated DNA from methylated cDNA was performed using an optical synthesized probe (thionine-based polymer). Hybridization of pDNA with various types of cDNA sequences was studied by UV-visible and fluorescence spectroscopy. Also, some mismatch sequences were applied as negative control. For this purpose, The synthesized optical probe were characterized by transmission electron microscopy, atomic force microscopy, dynamic light scattering, zeta potential, energy dispersive X-ray spectroscopy, Fourier transform infrared spectroscopy, UV-Vis, and fluorescence spectroscopy. Under optimal conditions, the analytical performance of engineered DNA-based assay was studied and exhibited excellent dynamic range (1 zM to 3 pM) with a low limit of quantitation (LLOQ) of 1 zM. The designed DNA-based assay showed a high capability of discriminating methylation, unmethylated, and mismatched sequences. The engineered genosensor is simple and inexpensive and can detect DNA methylation with high sensitivity. Therefore, the designed geno-assay could detect DNA methylation significantly and discriminate from unmethylated DNA.

2 | MATERIALS AND METHODS

2.1 | Chemicals and reagents

Potassium oxalate ($K_2C_2O_4$), Tris-HCl, and EDTA and 3,7-diaminophenothiazin-5-ium (thionine) were purchased from Sigma-Aldrich (Ontario, Canada). All the chemicals were analytical grade and used without any further purification. Deionized water was used in all solutions and experiments. The 24 bp oligonucleotide sequences used in the study were synthesized according to promoter area-specific sequence of APC gene by Takapouzist Co. (Iran) include:

- Probe sequence (pDNA): TCCGCTTCCCGACCCGCACTCCGC
- Complementary unmethylated sequence (target 1): GCGGAGTGC GGGTCGGGAAGCGGA;
- Complementary unmethylated sequence (target 2) with one base mismatched (unmethylated interferer CDNA): GCGGAGTAC GGGTCGGGAAGCGGA;
- Three base methylated sequences (target 3): GC(M)GGAGTGC(M) GGGTC(M)GGGAAGC(M)GGA
- Three base methylated sequences with one base mismatched (target 4) (methylated interferer CDNA): GC(M)GGAGTAC(M)GGGTC (M)GGGAAGC(M)GGA;

All oligonucleotides stock solutions were diluted with Tris-HCl-EDTA (TE) buffer. Blood plasma was obtained by the Blood Transfusion Institute from the blood of healthy individuals.

2.2 | Apparatus

The fluorescence measurements were performed using a Perkin Elmer PF-750 spectrofluorometer (Japan) equipped with 1.0 cm quartz cells

and a 150 W xenon lamp. The size and zeta potential of polymer were measured using Zetasizer instrument v.7.11 (Malvern Instruments Ltd). The pattern was recorded in the two theta range from 20 to 80. The UV-Vis absorption spectra were measured at room temperature on a Shimadzu UV-1800 UV-VI spectrophotometer with a resolution of 1 nm. The morphology of the optical probe was characterized by transmission electron microscopy (TEM) using a Philips CM30 electron microscope operated at 200 kV (Adelaide, Australia) and atomic force microscopy (AFM). The Fourier transform infrared (FT-IR) spectra were recorded by a Vector-22 BRUKER spectrophotometer (Switzerland). The electrode surface morphology was characterized by a high-resolution field emission scanning electron microscope (FE-SEM, Hitachi-SU8020, Czech) with an operating voltage of 3 kV, and chemical compositions of the electrode were analyzed by an energy dispersive spectroscopy (EDS) coupled with the FE-SEM equipment.

2.3 | GENERAL PROCEDURES

2.3.1 | Synthesis of the optical probe

To synthesize the optical probe, 5 mL of 5 mM thionine solution was mixed with 5 mL of 2 mM potassium oxalate solution. The resulting solution was sonicated for 30 minutes at 30°C, and after centrifugation and washing with deionized water, the resulting solution was dispersed in deionized water and stored at 4°C. Negatively charged oxalate ions act as a thionine reductant and stabilizer, reacting with the thionine amine group to form a polymer. Oxalate ions affect polymer growth by combining with positively charged thionine. Potassium oxalate is converted to oxalate anions in the aquatic environment and form hydrogen bonds with water molecules. The addition of thionine disrupts hydrogen bonds, and an electrostatic interaction is formed between thionine the oxalate ions (Scheme 2). This solution was synthesized and used daily.

2.3.2 | Fabrication of genosensor

Hybridization reaction performed at a total volume of 200 μL contains polymer and pDNA 10^{-13} M concentration. The resulting mixture was incubated for 15 minutes at 37°C. Then, different concentrations (10^{-21}, 10^{-18}, 10^{-15}, 0.1×10^{-12}, 0.2×10^{-12}, 0.3×10^{-12} M) of the methylated and unmethylated target oligonucleotide (cDNA) and NaCl (0.2 M) were then gently added into the mixture. The resulting mixture was incubated at 37°C for 15 minutes. Finally, the DNA hybridization detection was performed using UV-visible and fluorescence spectroscopic methods. Also, no color change was observed after adding pDNA and cDNA to the solution to the optical probe (Figure 1).

The heterocyclic and π-rich structure of thionine makes thionine-derived compounds able to interact with pDNA molecules through π-π stacking. The ring structure of thionine as a potent fluorophore has fluorescence properties that can show fluorescence properties at a specific wavelength. Also, due to the presence of NH_2 groups on both sides of thionine structure as electron donor groups causes the π electrons to become decentralized. Therefore, these groups increase the fluorescence property of thionine.

Thionine can be intercalated between DNA base pairs due to its fused heterocyclic structure. Because thionine has a maximum absorption spectrum at a wavelength of 598 nm, when it is combined with different concentrations of DNA, its significant hypochromic and bathochromic effects are observed at this wavelength that indicates a strong intermolecular interaction of π-π.[34] Thus, in the case of intercalating drugs, the molecules are inserted into the base stack of the helix. The rotation of free molecules contributes to the radiationless deactivation of the excited states, but if the drugs are bound to DNA, the deactivation via fluorescence emission is obtained, and a significant increase in the fluorescence emission is normally observed.[35]

3 | RESULTS AND DISCUSSION

3.1 | DLS, Zeta potential, EDS, FT-IR analysis of optical probe

DLS (dynamic light scattering) analysis was used to determine the particle size of the optical probe. Accordingly, the hydrodynamic radius of the optical probe and their dispersion index were evaluated. The average particle size of the synthesized polymer was 200 nm and the polydispersity index (PDI) was 10.25, which indicates the variation in the size of the synthesized polymer particles (Figure 2). The chemical composition of the optical probe was analyzed by EDS (Figure 3).

FT-IR spectra were used to analyze the composition of the optical probe (Figure 4). In FT-IR spectra of the optical probe, two bands 1316 and 1386 cm^{-1} related to the symmetric stretching frequency of (C-O) bonds and peak at 1608 cm^{-1} related to asymmetric bond (C-O)[36] (curve a) and the peak at 3410 cm^{-1} related to the hydroxyl group of the carboxylic acid of potassium oxalate. Compared with the spectrum of potassium oxalate, the intensity and position of the peak

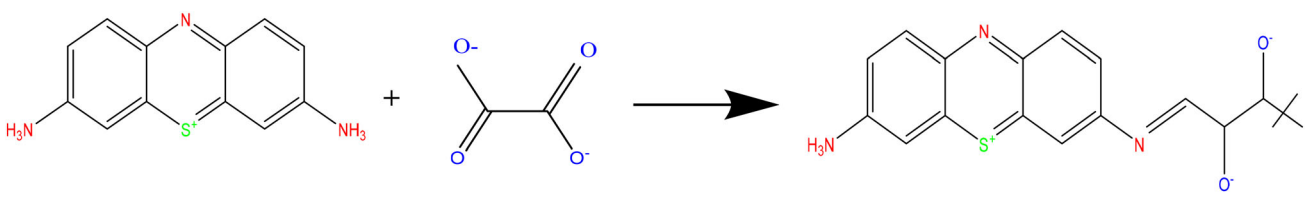

SCHEME 2 Combination mechanism of thionine with oxalate

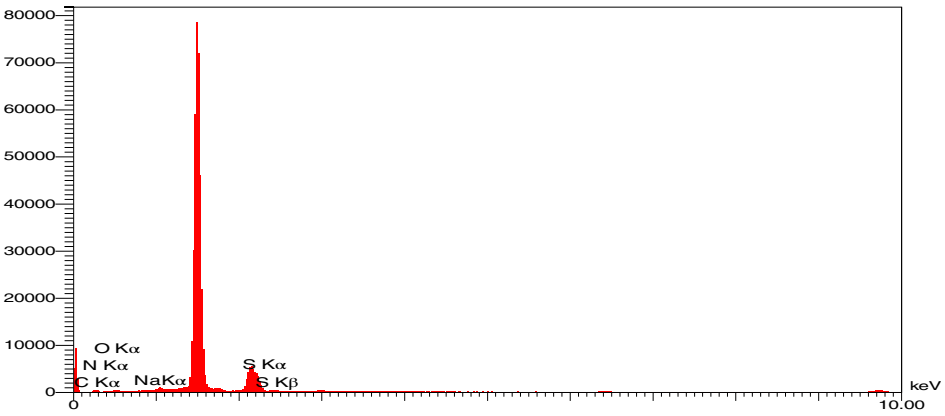

FIGURE 2 Size distribution analysis of optical probe

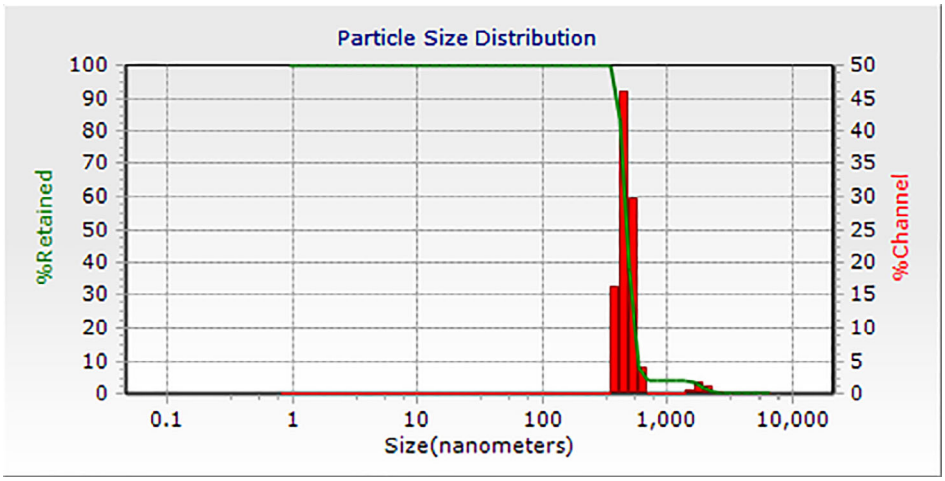

FIGURE 3 EDS spectra of the optical probe

at 1608 cm^{-1} was changed in the IR spectrum of the optical probe, which can be attributed to the integration of this peak with C=N bond in the optical probe (curve A).[37] The absorption bands at 3000 cm^{-1} of monomeric thionine (curve C), attributed to the symmetric stretching vibrations of -NH2 and disappeared in polymer, which reveals that the amine groups are reacting with oxalate.[38,39]

3.2 | Morphological characterization of the optical probe

The shape, size, and morphology of the synthesized probe were determined by TEM, FE-SEM, and AFM images (Figure 5). The polymer appeared nearly spherical and had an average diameter between 50 and 200 nm. The increase in the diameter of some polymer nanoparticles could be due to the aggregation of several polymer nanoparticles. The TEM image of a single optical probe showed the spherical shape (Figure 5B).

3.3 | Optimization of hybridization time

To obtain the optimum reaction time of the pDNA with DNA hybridization reaction, a certain volume of the optical probe was mixed with the pDNA. Then the methylated or unmethylated cDNA and NaCl (0.2 M) were added. The resulting solution was incubated for different time periods (15, 30, 45, 60, and 75 minutes). Then, UV-Vis absorption and fluorescence emission spectra were recorded. The results showed that the optimum reaction time between pDNA and cDNA was at 15 minutes (Figure 6). In 15 minutes, the adsorption peak of methylated cDNA was lower than non-methyl cDNAs.

3.4 | Analytical evaluation of genosensor

To evaluate the designed genosensor, different concentrations (10^{-21}, 10^{-18}, 10^{-15}, 0.1×10^{-12}, 0.2×10^{-12}, 0.3×10^{-12} M) of cDNA were used in the hybridization reaction with pDNA and optical probe. Then, the reaction solution was incubated for 15 minutes at 37°C. As shown in Figure 7, the maximum absorption peak was recorded for a concentration of 10^{-21} M, and the absorption peak was decreased with increasing concentrations of cDNA. Therefore, according to the obtained results, the designed genosensor can detect cDNA with a concentration of 10^{-21} M for both UV-Vis spectrophotometer and fluorescence spectroscopic techniques, and regression equations recorded for both systems were as follows:

$$\mathrm{Ab} = -0.0217\,(-\log C_{\mathrm{cDNA}}) + 2.3581, R^2 = 0.8386\,(\mathrm{by\,UV-Vis})$$

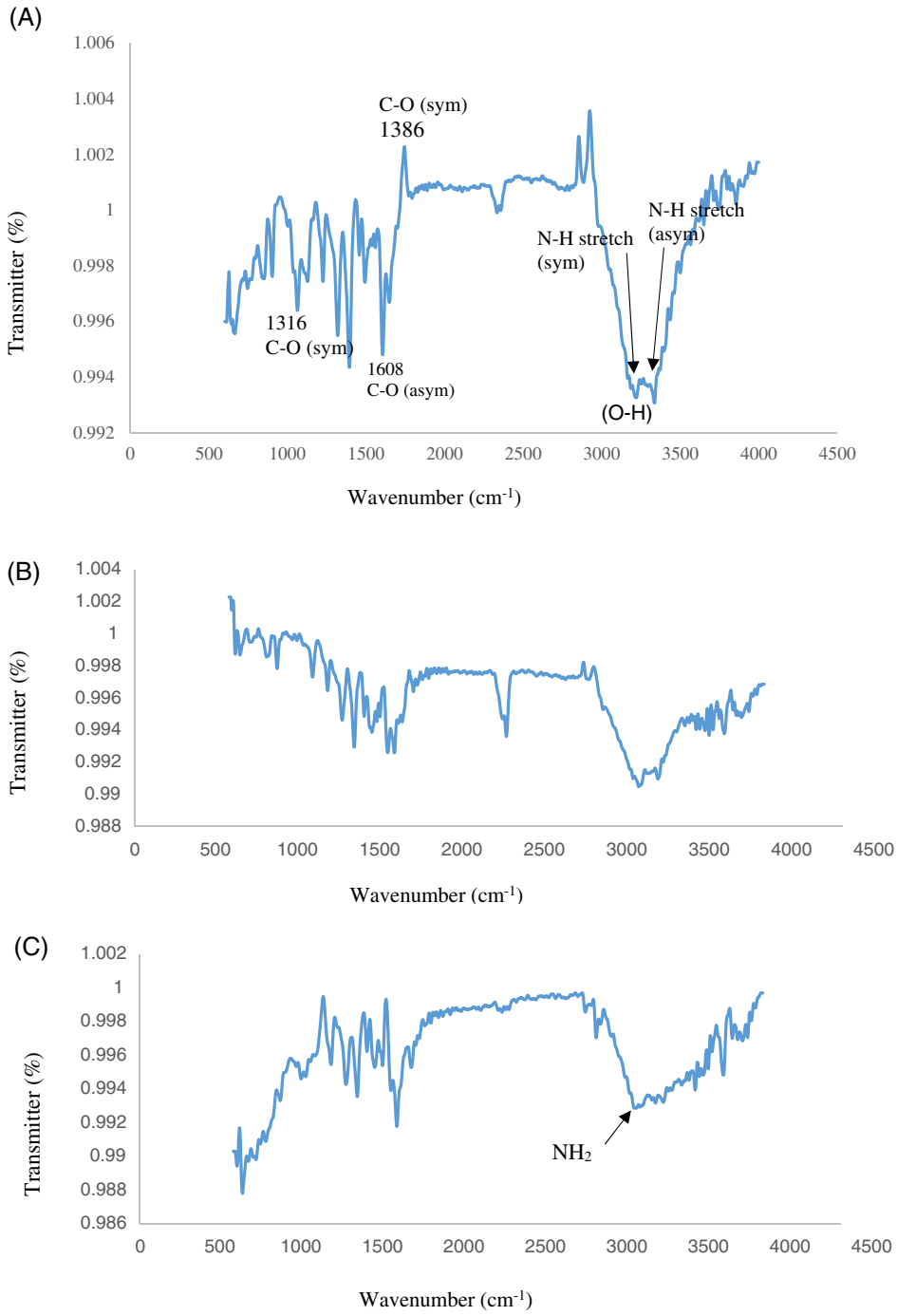

FIGURE 4 A, FT-IR spectra of the optical probe, B, oxalate potassium, C, thionine

and

$$\text{Int} = -2.6433\,(-\log C_{\text{cDNA}}) + 98.691, R^2 = 0.8027\,(\text{By fluorometry}).$$

The LLOQ of the designed nanobiosensor in the present study was 10^{-21} M, which indicates the high sensitivity of the nanobiosensor for differentiating methylated cDNA (GC(**M**)GGAGTGC(**M**)GGGTC(**M**)GGGAAGC(**M**)GGA) from unmethylated (GCGGAGTGCGGGTCGGGAAGCGGA) one. Comparing our analytical results with previous reports, Table 1 was prepared. The literature review indicated that Dadmehr and colleagues had designed a fluorometric nanobiosensor with a detection limit of 3.1×10^{-16} M.[40] Also, Rafiei and et al conducted a fluorometric study to detect DNA methylation, and the synthesized biosensor had a detection limit of 73 pM.[41] Also, Houang et al, used a labeled electrochemical method to differentiate methyl from unmethylated with a detection limit of 10^{-15} M,[42] and interestingly, Safarzadeh and coworkers used a label-free electrochemical immunosensor method with a detection limit of 12 f M to differentiate methylated sequences from the unmethylated.[43] According to the results of the mentioned research studies, in the present study, the low detection limit of the nanobiosensor shows the high sensitivity and efficiency of this nanobiosensor in differentiating methylated sequence from the unmethylated sequence (Table 1).

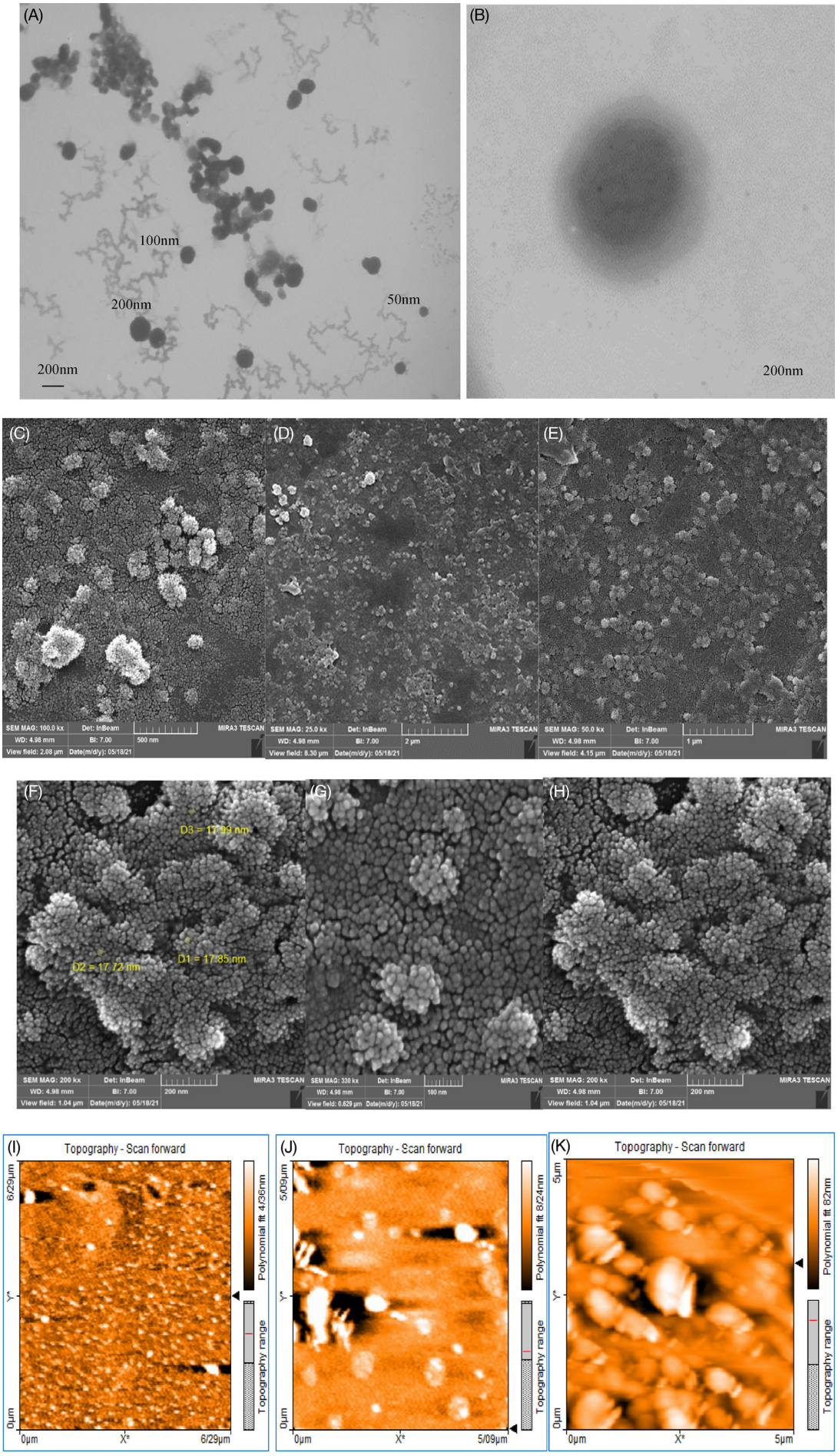

FIGURE 5 TEM images of the optical probe A, TEM image of a single thionine polymer B, FE-SEM images of the optical probe C-H, AFM images of the optical probe I-K

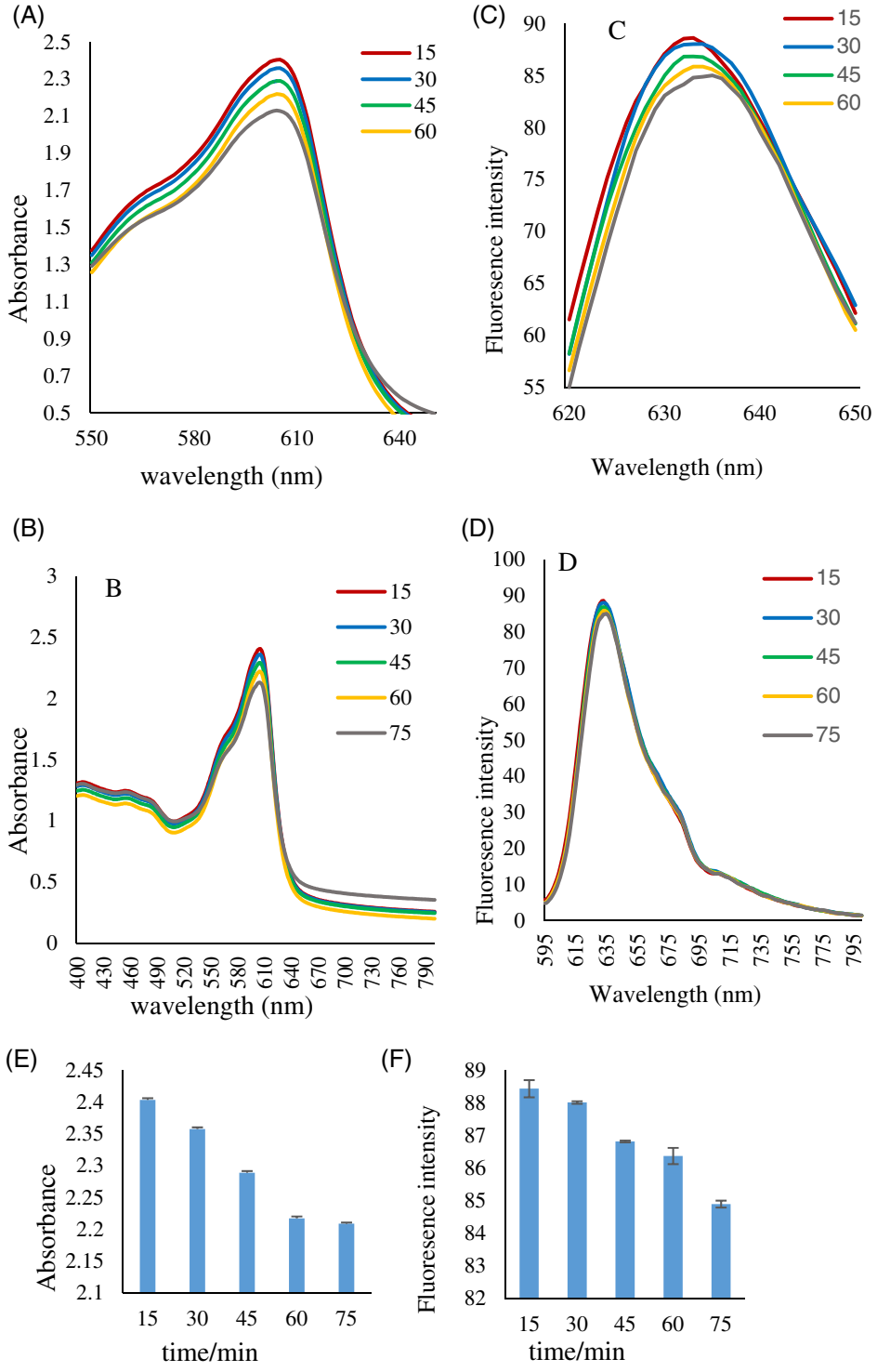

FIGURE 6 UV-Vis absorption A,B, and fluorescence excitation spectra C,D, of genosensor in various hybridization times (15, 30, 45, 60, 75 minutes). E,F, Histogram of peak intensity vs time of incubation

3.5 | Specificity and selectivity of genosensor

To evaluate specificity and selectivity of the optical probe, the bio-receptor (conjugation probe-pDNA) was hybridized with different methylated and unmethylated cDNAs and was evaluated using UV-Vis absorbance and fluorescence intensity under optimal conditions (Figure 8). It could be clearly observed that the UV-Vis and fluorescence intensity decreased gradually by increasing the concentrations of unmethylated interferer cDNA, unmethylated cDNA, methylated interferer cDNA, methylated cDNA sequence, respectively (1.94, 1.85, 1.79, 1.72 for UV-Vis, and 92.91, 88.68, 85.51, 80.28 for fluorescence). The decrease of UV-Vis absorption and fluorescence intensity observed with methylated sequences compared with unmethylated sequences can be attributed to methyl groups. By increasing the concentration of cDNAs (methylated and unmethylated), a slight decrease was observed in UV-Vis absorption

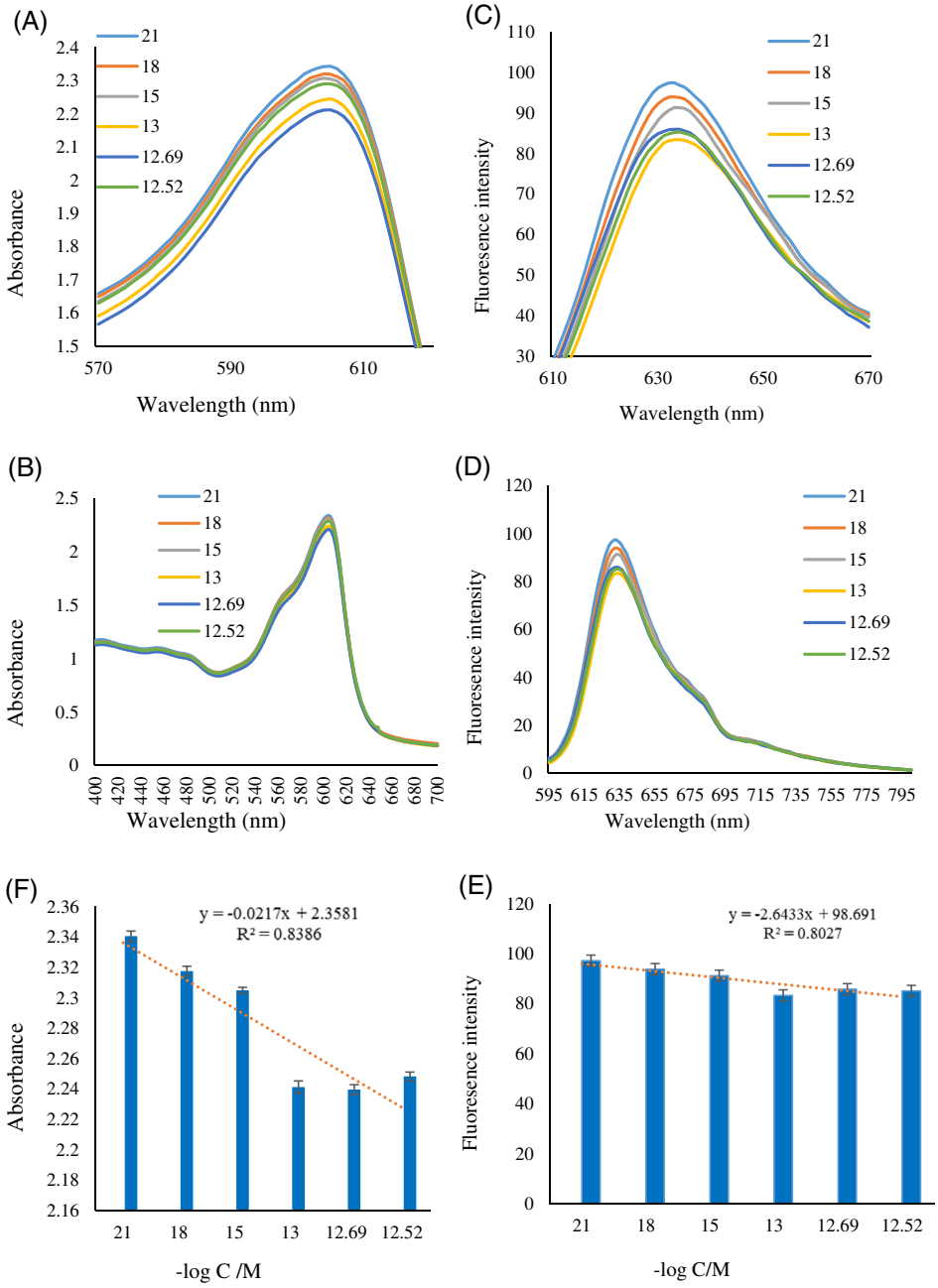

FIGURE 7 UV-Vis A,B, and fluorescence spectra C,D, of biosensor after hybridization with different concentrations of cDNA (10^{-21}, 10^{-18}, 10^{-15}, 0.3×10^{-12} M). Histograms of peak intensity vs concentration of cDNA E,F

TABLE 1 Comparison of different biosensing strategies for identification of DNA methylation

Method	Linear range/M	LOD/LLOQ	Reference
Fe_3O_4/Au core/shell fluorometric method	3.2×10^{-15} to 8.0×10^{-13}	0.3 fM	40
Label-free fluorometric method	10^{-10} to 10^{-6}	73 pM	41
Labeled electrochemical method	10^{-15} to 10^{-8}	1 fM	42
Label-free electrochemical immunosensor	50×10^{-15} to 100×10^{-12}	12 fM	43
Fluorometric nanobiosensor	0.3×10^{-12} to 10^{-21}	1 zM (LLOQ)	This study

and fluorescence (Figure 8). These results illustrated that the optical probe distinguishes between methylated and unmethylated DNA sequences. Also, this optical probe can detect sequences that contain mismatches. So it could be deduced that the presence of methyl groups as an electron-donating group on the methylated hybridized DNA may cause the possible changes in orientation, the intercalation, and interaction of thionine with DNA and decreases the fluorescence intensity rather than unmethylated DNA.

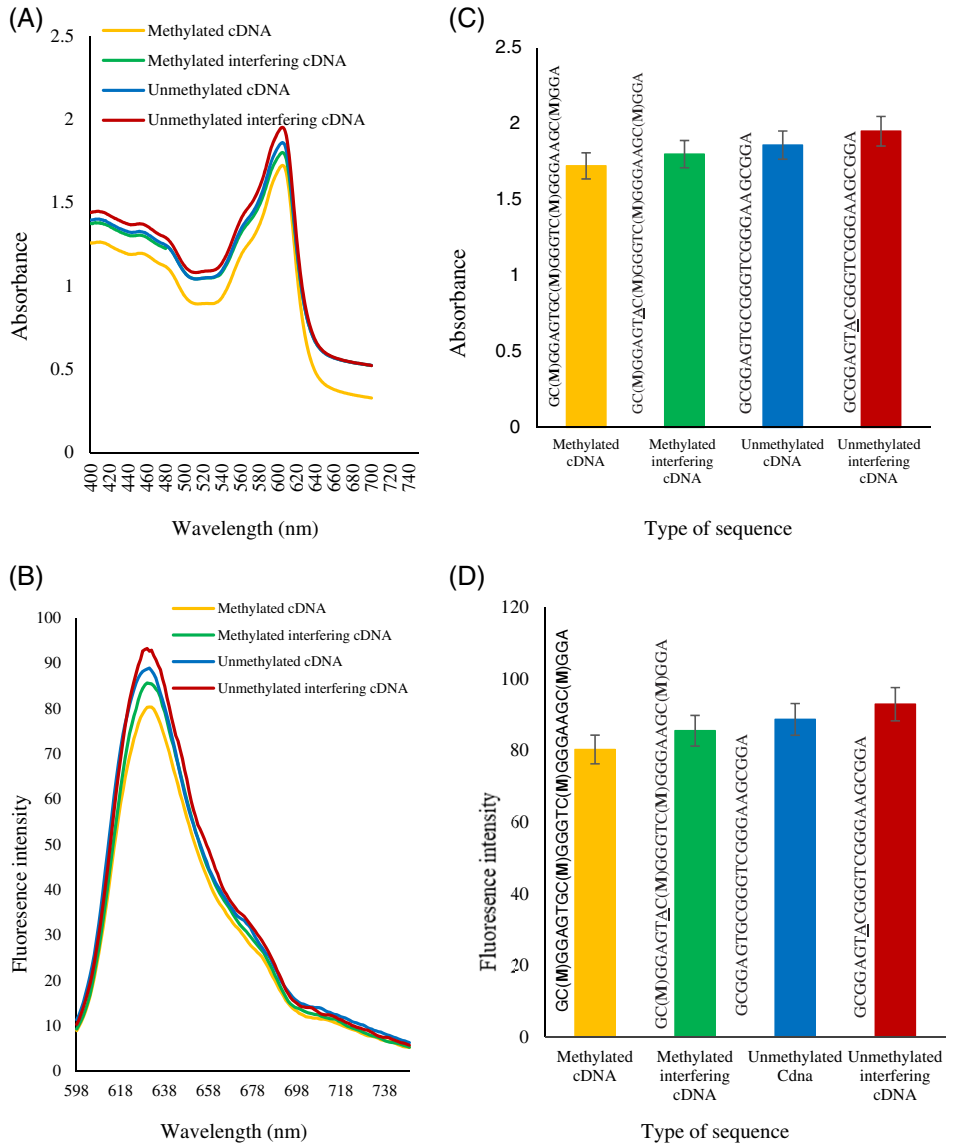

FIGURE 8 UV-Vis A, and fluorescence excitation B, of the optical probe, pDNA and hybridization of pDNA with methylated cDNA, methylated interfering cDNA, unmethylated cDNA, unmethylated interfering cDNA. Histograms of peak intensity vs type of sequence C,D

4 | CONCLUSION

In the current study, the DNA methylation was evaluated based on a sensitive and novel fluorometric genosensor. The interaction between pDNA with methylated and unmethylated cDNA was investigated in the presence of an engineered genosensor using UV-Vis and fluorescence spectroscopy. The presence of synthesized genosensor has been investigated with UV-Vis and fluorescence spectroscopy. The results showed that the proposed genosensor could differentiate methylated DNA from unmethylated DNA. The genosensor can also detect a mismatch in the DNA sequence along with the distinguishing of methyl groups. Therefore, the designed genosensor has a dual function. The UV-Vis absorbance and fluorescence intensity of unmethylated DNA were higher than that of methylated DNA. UV-Vis absorbance and fluorescence intensity were also higher at lower concentrations of cDNA than at higher concentrations. The UV-Vis absorbance and fluorescence intensity of the optical probe and optical probe/pDNA showed slight difference at different times. The detection limit of the genosensor was 10^{-21} M, and the duration was 15 minutes, and the linear range was 1 zM to 0.3 pM. This genosensor can also detect methylation in plasma samples. Finally, this genosensor provides a rapid, simple, and sensitive method to evaluate methylation in the early stages of methylation-related diseases such as cancer.

ACKNOWLEDGEMENTS

The researchers thank the University of Tabriz and University of Tabriz of Medical Science for financial support of this research.

DATA AVAILABILITY STATEMENT

The data that support the findings of this study are available on request from the corresponding author. The data are not publicly available due to privacy or ethical restrictions.

ORCID

Gholamreza Dehghan https://orcid.org/0000-0002-7813-5226

Mohammad Hasanzadeh https://orcid.org/0000-0003-4918-1239

REFERENCES

1. Anand P, Kunnumakkara AB, Kunnumakara AB. Cancer is a preventable disease that requires major lifestyle changes. *Pharm Res*. 2008; 25:2097-2116.
2. Holliday R. Cancer is a preventable disease that requires major lifestyle changes. *Science*. 1987;238:163-170.
3. Bird A. DNA methylation patterns and epigenetic memory. *Genes Dev*. 2002;16:6-21.
4. Kristensen LS, Nielsen HM, Hansen LL. DNA methylation patterns and epigenetic memory. *Eur J Pharmacol*. 2009;625:131-142.
5. Klose RJ, Bird AP. Genomic DNA methylation: the mark and its mediators. *Trends Biochem Sci*. 2006;31:89-97.
6. Stoccoro A, Karlsson HL, Coppede F, Migliore L. Epigenetic effects of nano-sized materials. *Toxicology*. 2013;313:3-14.
7. Kasinski AL, Slack FJ. Epigenetics and genetics. MicroRNAs en route to the clinic: progress in validating and targeting microRNAs for cancer therapy. *Nat Rev Cancer*. 2011;11:849-864.
8. Roosbroeck KV, Pollet J, Calin GA. MicroRNA biomarkers for early detection of embryonic malformations in pregnancy. *Expert Rev Mol Diagn*. 2013;13:183-204.
9. Bestor TH. Cloning of a mammalian DNA methyltransferase. *Gene*. 1988;74:9-12.
10. Zhang GQ, Esteve PO, Chin HG, et al. Allosteric control of mammalian DNA methyltransferases – a new regulatory paradigm. *Nucleic Acids Res*. 2015;43:6112-6124.
11. Straussman R, Nejman D, Roberts D, Steinfeld I, Blum B, Benvenisty N. Developmental programming of CpG island methylation profiles in the human genome. *Mol Biol*. 2009;16:564-571.
12. Robertson KD. DNA methylation and human disease. *Nat Rev Genet*. 2005;6:597-610.
13. Smith ZD, Meissner A. DNA methylation: roles in mammalian development. *Nat Rev Genet*. 2013;14:204-220.
14. Paska AV, Hudler P. Current cancer drug targets. *Curr Cancer Drug Targets*. 2018;18:65-88.
15. Esteller M. Relevance of DNA methylation in the management of cancer. *Lancet Oncol*. 2003;4:351-358.
16. Heyn H, Esteller M. DNA methylation profiling in the clinic: applications and challenges. *Nat Rev Genet*. 2012;13:679-692.
17. Bird AP. Use of restriction enzymes to study eukaryotic DNA methylation: II. The symmetry of methylated sites supports semi-conservative copying of the methylation pattern. *Mol Biol*. 1978;118:49-60.
18. Frommer M, McDonald LE, Millar DS. A genomic sequencing protocol that yields a positive display of 5-methylcytosine residues in individual DNA strands. *Proc Natl Acad Sci U S A*. 1992;89:1827-1831.
19. Mehri P, Pashazadeh-Panahi P, Hasanzadeh M, Razmi N. An innovative genosensor for the monitoring of Leishmania spp sequence using binding of pDNA to cDNA based on Cit-AgNPs. *Heliyon*. 2020;6(8): e04638.
20. Bahavarnia F, Pashazadeh-Panahi P, Hasanzadeh M, Razmi N. DNA based biosensing of Acinetobacter baumannii using nanoparticles aggregation method. *Heliyon*. 2020;6(7):e04474.
21. Hassanpour S, Saadati A, Hasanzadeh M. pDNA conjugated with citrate capped silver nanoparticles towards ultrasensitive bio-assay of haemophilus influenza in human biofluids: A novel optical biosensor. *J Pham Biomed anal*. 2020;180:113050.
22. Bahavarnia F, Mobed A, Hasanzadeh M, Saadati A, Hassanpour S, Mokhtarzadeh A. Bio-assay of Acintobacter baumannii using DNA conjugated with gold nano-star: A new platform for microorganism analysis. *Enzyme Microb Tech*. 2020;133:109466.
23. Adampourezare M, Dehghan G, Hasanzadeh M, Feizi MAH. Application of lateral flow and microfluidic bio-assay and biosensing towards identification of DNA-methylation and cancer detection: Recent progress and challenges in biomedicine. *Biomed Pharmacotherapy*. 2021; 141:111845.
24. Serrano NR, Rai-Constapel V, Daza MC, Doerr M, Marian M. Internal heavy atom effects in phenothiazinium dyes: enhancement of intersystem crossing via vibronic spin–orbit coupling. *Phys Chem Chem Phys*. 2015;17:11350-11358.
25. Tuite EM, Kelly JM. Photochemical interactions of methylene blue and analogues with DNA and other biological substrates. *J Photochem Photobiol*. 1993;21:103-124.
26. Jockusch S, Lee D, Turro NJ, Leonard EF. Functional Nanocomposites Based on Quantum Dots. *Proc Natl Acad Sci U S A*. 1996;93:7446-7451.
27. Dohno C, Stemp ED, Barton JK. Long-range electron and hole transport through DNA with tethered cyclometalated iridium(III) complexes. *J Am Chem Soc*. 2003;125:9586-9587.
28. Xu Y, Yang L, Ye X, He P, Fang Y. Impedance-based DNA biosensor employing molecular beacon DNA as probe and thionine as charge neutralizer. *Electroanalysis*. 2006;18:873-881.
29. Tuite EM, Kelly JM. Clinical tolerance of methylene blue virus–inactivated plasma. *Biopolymers*. 1995;35:419-433.
30. Chang TC, Yang YP, Huang KH, Chang CC, Hecht C. Investigation of thionin-DNA interaction by satellite hole spectroscopy. *Opt Spectrosc*. 2005;98:655-660.
31. Hecht C, Friedrich J, Chang TC. An electrochemical aptasensor for Pb2+ detection based on metal–organic-framework-derived hybrid carbon. *J Phys Chem*. 2004;108:10241-10244.
32. Hecht C, Hermann P, Friedrich J, Chang CC, Chang TC. Recombination zone in mixed-host organic light-emitting devices. *Chem Phys Lett*. 2005;413:335-341.
33. Ding Y, Zhang X, Liu X, Guo R. Adsorption characteristics of thionine on gold nanoparticles. *Langmuir*. 2006;22:2292-2298.
34. Paul P, Hossain M, Yadav R, Kumar GS. Biophysical studies on the base specificity and energetics of the DNA interaction of photoactive dye thionine: spectroscopic and calorimetric approach. *Biophys Chem*. 2010;148:93-103.
35. Gonzalez-Ruiz V, Olives AI, Martin MA, Ribelles P. An overview of analytical techniques employed to evidence drug-DNA interactions. Applications to the design of genosensors. *Biomed Eng Trends Res Technol*. 2011;10:65-90.
36. Gabal M, El-Bellihi A, Ata-Allah S. Effect of calcination temperature on Co(II) oxalate dihydrate–iron(II) oxalate dihydrate mixture: DTA–TG, XRD, Mössbauer, FT-IR and SEM studies (Part II). *Mater Chem Phys*. 2003;81:84-92.
37. Guo L, Wu S, Zeng F, Zhao J. Luminescence modulation of carbon dots assemblies. *Eur Polym J*. 2006;42:1670-1675.
38. Nath N, Sarker S, Rahman MM, Lee HJ. A facile template-free chemical synthesis of poly (thionine) nanowires. *Chem Phys Lett*. 2013;559: 56-60.
39. Liu SG, Luo D, Li N, et al. Water-soluble nonconjugated polymer nanoparticles with strong fluorescence emission for selective and sensitive detection of nitro-explosive picric acid in aqueous medium. *ACS Appl Mater Interfaces*. 2016;8:21700-21709.
40. Dadmehr M, Hosseini M, Hosseinkhani S, et al. A fluorometric study on the effect of DNA methylation on DNA interaction with graphene quantum dots. *Biosens Bioelectron*. 2014;60:35-44.
41. Rafieia S, Dadmehrb M, Hosseinia M, Ahmadzade Kermania H, Ganjali M. A fluorometric study on the effect of DNA methylation on

DNA interaction with graphene quantum dots. *Methods App Fluores*. 2019;7.
42. Huanga J, Zhang S, Moc F, Sud S, Chend X, Lia Y. A microfluidic biosensor for online and sensitive detection of Salmonella typhimurium using fluorescence labeling and smartphone video processing. *Biosens Bioelectron*. 2019;127:155-160.
43. Safarzadeh M, Suhail A, Sethi J, Sattar A, Jenkins D. A Label-free DNA-immunosensor based on aminated rGO electrode for the quantification of DNA methylation. *Nanomaterials*. 2021;4.

How to cite this article: Adampourezare M, Dehghan G, Hasanzadeh M, Feizi M-AH. Identification of DNA methylation by novel optical genosensing: A new platform in epigenetic study using biomedical analysis. *J Mol Recognit*. 2021;34(12):e2938. doi:10.1002/jmr.2938